The Composite Insertion Electrode

Atlung, Sven; Zachau-Christiansen, Birgit; West, Keld ; Jacobsen, Torben

Published in:
Journal of The Electrochemical Society

Link to article, DOI:
10.1149/1.2115778

Publication date:
1984

Document Version
Publisher's PDF, also known as Version of record

The Composite Insertion Electrode

Theoretical Part. Equilibrium in the Insertion Compound and Linear Potential Dependence

S. Atlung,* B. Zachau-Christiansen, K. West, and T. Jacobsen*

Fysisk-Kemisk Institut, The Technical University of Denmark, DK 2800 Lyngby, Denmark

ABSTRACT

The specific energy obtainable by discharge of porous insertion electrodes is limited by electrolyte depletion in the pores. This can be overcome using a solid ion conductor as electrolyte. The term "composite" is used to distinguish these electrodes from porous electrodes with liquid electrolyte. The theoretical basis for such electrodes is discussed and, using a simplified model, equations are derived to describe the distribution of potential and current during discharge/charge operation. Under the assumption that the insertion compound particles are small enough to ensure equilibrium, and that the local electrode potential depends linearly on the degree of insertion, these equations are solved to obtain analytical expressions for the discharge curve. It is shown that the parameters which determine the discharge behavior for a given discharge current are simply related to the effective ionic and electronic conductivities, the thickness of the electrode, the volume fractions, and the slope of the potential curve.

From a specific energy point of view, batteries with insertion electrodes have the advantage that the overall cell process

$$n\mathrm{M} + \mathrm{H} \rightarrow \mathrm{HM}_n \qquad [1]$$

only includes a minimum of components, and no changes in overall electrolytic composition.

The reaction at the positive electrode

$$\delta\mathrm{M}^+ + \delta e^- + \mathrm{HM}_x \rightarrow \mathrm{HM}_{x+\delta} \qquad [2]$$

is a topochemical reaction where the monovalent cation M^+ is inserted in the "host compound," H. δ is an infinitesimal increment in the degree of insertion x and the compound HM_x, for $x \leq n$, forms a single phase.

Hence Eq. [2] can take place in both directions with a minimum of structural changes. This should make it possible to design secondary batteries with long cycle life. Li is the metal most used for this type of batteries, but Eq. [2] is known to occur with Na^+ (1), K^+ (2), and Ag^+ (3) as well.

Many insertion compounds are known primarily from the groups of dichalcogenides (4), but lately also oxides, in particular, vanadium oxides, have been studied (5).

Based on the Li/TiS_2 couple, practical battery investigations have shown (6-8) that a specific energy in the range of 100-150 Wh/kg is a realistic goal for moderate temperature batteries. This can be compared with the 50-60 Wh/kg goal for advanced lead acid systems.

The limitations met with in the design of insertion compound batteries originate primarily from the low mobility of the M^+ cation in the electrolytes used (9). Alkali metal anodes dictate the use of nonaqueous electrolytes, either organic solvents with a M salt (10), or solid ionic conductors (7).

The dynamics of insertion cathodes.—Equation [2] is basically a solid-state reaction, whose rate is controlled by diffusion of M^+ into the insertion compound particle. This type of electrode kinetics has been discussed in relation to battery performance in earlier papers (11, 12). It was concluded that insertion cathodes should be made with small particles arranged in a porous structure in order to obtain acceptable specific energies at heavy loads. In a porous electrode, the utilization of the active materials depends on the transport in the active particles, electrode porosity and thickness, and electrolyte properties. By choosing small enough cathode particles, the influence of transport in these can be eliminated without impairing the packing density (11). For example, in the case of the Li/TiS_2 system, a particle size smaller than 1-2 μm ensures that even for 2-4h loads, the Li concentration in the particles is practically uniform.

The impedance for the interfacial charge transfer reaction can be assumed negligible for insertion reactions (13) and, accordingly, reaction [2], under these circumstances, proceeds close to equilibrium. Hence, the obtainable material utilization in the porous cathode is limited by transport phenomena in the electrolyte in the pores.

These problems were discussed in a previous publication (14), where it was concluded that the utilization of a porous cathode, designed for maximum energy density, was limited by local depletion of electrolyte salt in the cathode. This depletion occurs when the local transfer current consumes more M^+ ions than the amount supplied by diffusion and migration. In Ref. (12) it was indicated that the electrolyte depletion was a consequence of the transport of the anion and could be delayed or suppressed if the anion mobility was low enough. Thus, a low anion and a high cation mobility should be beneficial for material utilization. However, one might fear that the corresponding decrease in conductivity and the appearance of "diffusion potentials" would offset the gain.

A quantitative study was undertaken in Ref. (14) from which Fig. 1 is reproduced. It is obvious from this figure that the electrode performance is dramatically improved by decreasing anion mobility to a low value, regardless of the increase in electrolyte resistance. This points to the use of solid ion conductors with only one ionic species mobile as electrolytes in "porous" electrodes. To indicate the difference between electrodes with liquid electrolytes and solid electrolytes, the term "composite electrodes" is coined to describe these "all solid-state" electrodes.

Composite Electrodes

In experiments with solid ionic conductors it has been the practice to mix the electrode substance with electrolyte powder (15). So far no discussion of this procedure and the expected advantages is found in the literature.

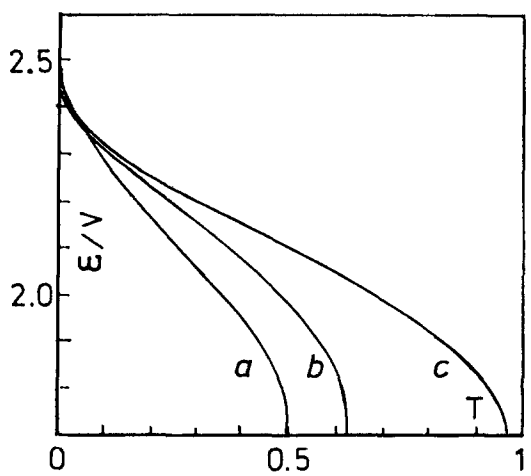

Fig. 1. Calculated discharge curves for porous electrode with liquid electrolyte. Cationic mobility kept constant, different values of t (a, b, c). a = 0.8, b = 0.1, and c = 0.01. For further details see Ref. (14).

*Electrochemical Society Active Member.

Key words: electrode, insertion, solid state, discharge.

For reversible batteries, a composite electrode can hardly be imagined with other electrode systems than insertion compounds because participation of electrolyte compounds in the cell reaction would destroy the structure. Even with insertion compounds the volume changes associated with charge and discharge might cause difficulties. The composite electrode must be made by mixing powders of the insertion compound and the solid electrolyte and consolidating this mixture on a metal grid serving as current collector.

The structure of a composite electrode is shown in Fig. 2. It is essential that the insertion material and the electrolyte form two interwoven contiguous networks with maximum contact area, and that the number of voids or isolated particles is at a minimum. The realization of such a strutcure is difficult; it can, however, be facilitated using a "soft" electrolyte like LiI-Al_2O_3 (16) or a small amount of polymeric electrolyte (17) to improve the contact between electrolyte and electrode particles (18).

The composite electrode concept is an imperative prerequisite for the construction of an all solid-state battery system exploiting the advantages associated with electrolytes conducting only the inserted ion.

Such a system can be operated at a moderately increased temperature, 100°-150°C. In the first place, this improves the rather low conductivity of solid electrolytes at room temperature. Assuming an activation energy for ionic transport of 0.3 eV, raising the temperature from 25° to 150°C will improve the battery rate capability by a factor of five. Also, the rate of the insertion process will be improved permitting use of less "active" insertion compounds or larger particles.

Operation of organic electrolyte batteries at increased temperature has until now not been successfully demonstrated, partly from safety considerations, and partly due to the tendency for solvent intercalation in layered materials. It is obvious that the composite electrode should be combined with a layer of solid electrolyte as a separator. The most promising electrolyte materials, Li_3N and LiI-Al_2O_3, are thermodynamically stable against Li, and this, possibly in connection with the increased temperature, improves the cyclability of the Li electrode considerably (18).

From a construction point of view, the possibility of stacking a number of cells to a high voltage unit without serious containment problems should improve overall specific energy. Hence, the expected advantages associated with the composite electrode concept warrants a closer study of its theoretical and practical aspects.

Theoretical Treatment

Model description.—It is assumed that the electrode is a flat pellet of thickness, l, (Fig. 3). The length coordinate is z, with $z = 0$ at the current collector. The electrode potential, ϵ_C is measured at the current collector with reference to an electrode reversible to M^+ placed at $z = l$. π is the Fermi potential in the electronically conducting insertion compound and ϕ the Galvani potential in the electrolyte. Hence

$$\epsilon_C = \pi_0 - \phi_1 \qquad [3]$$

where $\pi_0 = \pi(z = 0)$ and $\phi_1 = \phi(z = l)$.

Due to the equivalence between the electrolyte and insertion compound, it is natural to use the macrohomogeneous model as introduced by Newman and Tobias (19). According to this model, each point is associated with local values of π, ϕ, ionic current density, i_l, and electronic current density, i_e. The electrochemical reaction causes a transfer current, i_t, measured per unit volume electrode. These variables are all functions of position, z, and time, t.

We further ascribe an effective electronic conductivity, κ_e, and a corresponding ionic conductivity, κ_l, to the electrode structure as such. These quantities then include the effect of tortuosity and volume fraction of the insertion and the electrolyte components, respectively. Neglecting volume changes due to charge/discharge, κ_l can be considered constant in time and space, when a true solid ionic conductor is used. This makes all the difference between the treatment of the composite and the porous electrode with liquid electrolyte, where composition and conductance of the electrolyte changes with time and position.

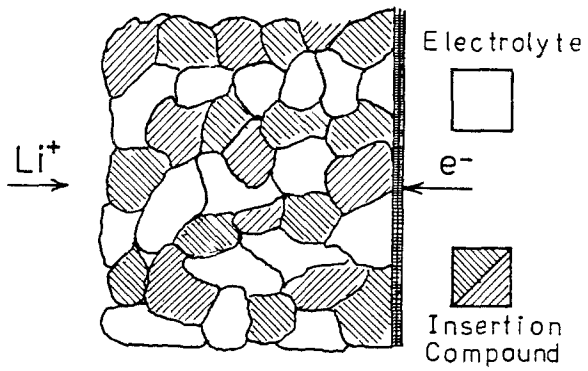

Fig. 2. Composite electrode concept (two dimensional)

For some insertion compounds, the electronic conductivity of the pure substance, κ_e^0, can change considerably with the amount of inserted ion. However, the effective value of κ_e in the electrode can be controlled by conducting additives like graphite, etc.

In the following, κ_e is considered constant, the interfacial charge transfer is assumed to be in equilibrium, and the local concentration of inserted ion in each insertion compound particle is uniform. Also, electrical gradients perpendicular to the Z-axis are assumed negligible. Under these assumptions, the transport equations are

$$i_l = -\kappa_l \frac{d\phi}{dz} \quad \text{and} \quad i_e = -\kappa_e \frac{d\pi}{dz} \qquad [4]$$

and the conservation of mass and charge requires

$$i_t = \frac{\partial i_l}{\partial z} \quad \text{and} \quad i_l + i_e = i^* \qquad [5]$$

i^* is the discharge/charge current density (counted negative for cathodic, *i.e.*, discharge currents). The local single electrode potential is given as

$$\epsilon = \pi - \phi \qquad [6]$$

and Eq. [4]-[6] give the porous electrode relation (20)

$$\frac{\partial^2 \epsilon}{\partial z^2} = i_t\left(\frac{1}{\kappa_l} + \frac{1}{\kappa_e}\right) \qquad [7]$$

with the boundary conditions for constant current discharge

$$z = 0,\ i_e = i^*;\ z = l,\ i_l = i^* \qquad [8]$$

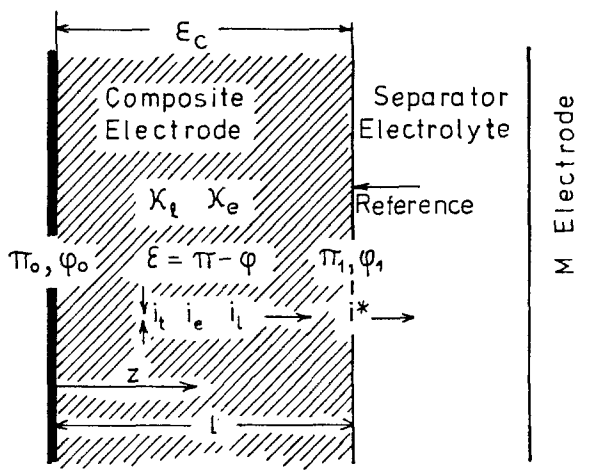

Fig. 3. Specification of composite electrode model

which on the strength of Eq. [4] and [5] can be written as

$$z = 0,\ \partial\epsilon/\partial z = -i^*/\kappa_e$$
$$z = l,\ \partial\epsilon/\partial z = i^*/\kappa_l \qquad [9]$$

The insertion electrode potential.—In porous and composite insertion electrodes, the reaction is distributed through the electrode, mainly as a result of the change in potential associated with the change in the local degree of insertion caused by the discharge/charge process. A characteristic for insertion compounds is that their equilibrium potential depends strongly on the degree of insertion. One example of this dependence is the relation proposed by Armand (21) for TiS_2/Li

$$\epsilon = \pi - \phi = \epsilon^\theta + RT/\mathbf{F}(\ln[(1 - X)/X] - f[X - 0.5]) \qquad [10]$$

where $X = x/n$ is the degree of insertion, f an "interaction parameter," and ϵ^θ a standard potential for the insertion compound/electrolyte in question.

The interaction parameter, f, expresses approximately the effect of the electrostatic interactions associated with the insertion process (23) and dominates the dependence of the potential on X. The typical range for the linear term is $10 < f < 20$, *e.g.*, 16 for TiS_2.

A relation of the form Eq. [10] presumes that the insertion takes place in a monophasic region. If, for example, new phases are formed during insertion, the EMF composition relation will exhibit plateaus, and relations like Eq. [10] are only valid within limited regions.

In Fig. 4, we have depicted the TiS_2/Li potential as measured (29) and calculated from Eq. [10]. In this case, it is obvious that a simple linear dependence

$$\epsilon = \epsilon^* - kX \qquad [11]$$

is a good approximation. Although other insertion compounds may show this behavior only in a limited range, it is believed that Eq. [11] brings out the characteristic features of insertion electrodes compared with other battery electrodes like HgO, AgCl, and PbO_2.

The working potential.—The working potential is given by Eq. [3]. In case of a significant contribution from the electronic resistance in the insertion compound network, ϵ_C cannot be identified with the local electrode potential

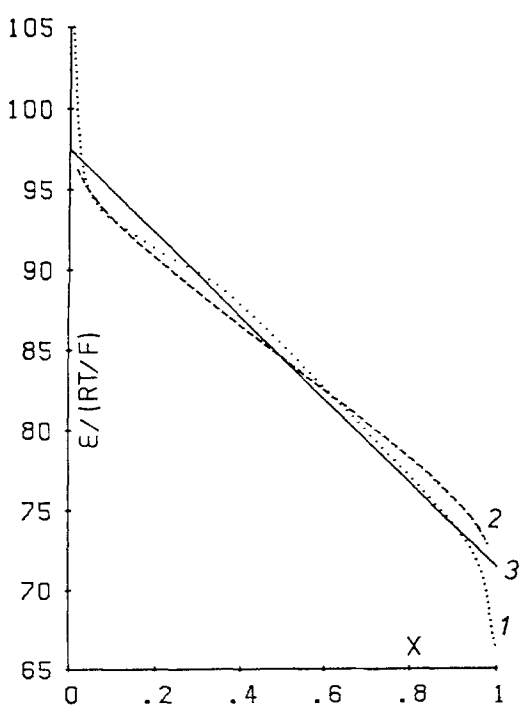

Fig. 4. Insertion electrode potential. (1) measured Ref. (29), (2) approximation according to Eq. [10], and (3) linear approximation (ϵ^* = 2.49V, k = 0.67V).

ϵ_l at $z = l$. Many insertion compounds have a high electronic conductance as, *e.g.*, TiS_2, while other compounds interesting from a battery point of view show a rather low electronic conductivity, *e.g.*, some of the vanadium oxides.

Until now there still remains some uncertainty as to the influence of electronic resistivity on battery performance, although it was a main topic in some of the first works on porous electrodes (24).

The following treatment is quite general and based on the local potentials: $\epsilon_l = \epsilon(z = l) = \pi_l - \phi_l$ and $\epsilon_o = \epsilon(z = 0) = \pi_o - \phi_o$. From Eq. [3], we have

$$\epsilon_C = \pi_o - \phi_l = \pi_l - \phi_l - (\pi_l - \pi_o) \qquad [12]$$

and from Ohms law (κ_e constant)

$$\pi_l - \pi_o = -\frac{1}{\kappa_e}\int_o^l i_e dz \qquad [13]$$

and using Eq. [4] and [7]

$$i_e = \int_z^l i_l dz = \frac{\kappa_e\kappa_l}{\kappa_e + \kappa_l}\int_z^l \frac{\partial^2\epsilon}{\partial z^2}\,dz \qquad [14]$$

Performing the integration and using the boundary conditions in Eq. [9] we obtain

$$\epsilon_C = \frac{1}{\kappa_e\kappa_l}(\kappa_e\epsilon_l + \kappa_l\epsilon_o + li^*) \qquad [15]$$

At this stage, it is convenient to introduce the parameters ϵ_l^o and ϵ_e^o to express the potential difference which would develop across the electrode, if all the current passed through the ionically conducting network or the electronically conducting network, respectively

$$\epsilon_l^o = -i^*l/\kappa_l;\ \epsilon_e^o = -i^*l/\kappa_e \qquad [16]$$

As it will appear later, these two parameters and k determine the behavior of the electrode over the entire discharge range. With these ϵ_C can be written as

$$\epsilon_C = \frac{\epsilon_l^o \cdot \epsilon_l}{\epsilon_l^o + \epsilon_e^o} + \frac{\epsilon_e^o \cdot \epsilon_o}{\epsilon_l^o + \epsilon_e^o} - \frac{\epsilon_l^o \cdot \epsilon_e^o}{\epsilon_l^o + \epsilon_e^o} \qquad [17]$$

The ratio $\beta = \epsilon_e^o/\epsilon_l^o = \kappa_l/\kappa_e$ expresses the influence of increasing the electronic resistance for a fixed value of the ionic resistance. Using β, we get

$$\epsilon_C = \frac{1}{1+\beta}\epsilon_l + \frac{\beta}{1+\beta}\epsilon_o - \frac{\beta}{1+\beta}\epsilon_l^o \qquad [18]$$

Mathematical treatment.—It is characteristic for porous and composite electrodes that the transport in the two phases is coupled through the local electrode potential $\epsilon = \pi - \phi$. As ϵ is given by the local value of X, which depends on the local degree of discharge, the time dependence of the electrode behavior is introduced. If, as assumed, the insertion compound particles are in equilibrium, then

$$\frac{\partial X}{\partial t} = -\frac{i_t}{\mathbf{F}vc^o} \qquad [19]$$

where c^o is the saturation concentration ($x = n$) and v is the volume fraction of insertion compound. Combining this with Eq. [7] and [16], we get

$$\frac{\partial X}{\partial t} = \frac{i^*l}{\mathbf{F}vc^o(\epsilon_e^o + \epsilon_l^o)}\,\frac{\partial^2\epsilon}{\partial z^2} \qquad [20]$$

For convenience, dimensionless variables and groups are introduced. For a battery discharge at constant current, the obvious time unit is the time needed to discharge the battery completely. At equilibrium conditions this is

$$\tau_D = -\mathbf{F}lvc^o/i^* \qquad [21]$$

keeping in mind that cathodic currents are negative. τ_D is the "stoichiometric" discharge time and can be consid-

ered a measure of the intensity of the discharge. Equivalent terminology is used in the battery industry, *e.g.*, a "5h load." The dimensionless time

$$T = t/\tau_D = -ti^*/\mathbf{F}lvc^o \qquad [22]$$

is then identical to the degree of discharge.

Introducing dimensionless length, Z, and potential, E

$$Z = z/l;\ E_j^m = \mathbf{F}\epsilon_j^m/RT;\ \text{and}\ K = \mathbf{F}k/RT \qquad [23]$$

transforms Eq. [20] and [9] into

$$\frac{\partial X}{\partial T} = -\frac{1}{E_l^o + E_e^o}\frac{\partial^2 E}{\partial Z^2} \qquad [24]$$

$$Z = 0,\ \partial E/\partial Z = E_e^o;\ Z = 1,\ \partial E/\partial Z = -E_l^o$$

where

$$E_j^o = \frac{\mathbf{F}^2 l^2 v c^o}{RT\tau_D \kappa_j}\ (j = e,l) \qquad [25]$$

and the potential relation in Eq. [10] into

$$E = E^\theta + \ln[(1 - X)/X - f(X - 0.5)] \qquad [26]$$

and Eq. [11]

$$E = E^* - KX \qquad [27]$$

Equations [24] and [26] or a corresponding potential relation form two simple nonlinear simultaneous second-order differential equations from which E or X can be found as functions of T and Z by well-known numerical methods. Here we will use the linear relation in Eq. [27] to obtain an analytical solution. Equations [24] and [27] give

$$\frac{\partial X}{\partial T} = \frac{K}{E_l^o + E_e^o}\frac{\partial X^2}{\partial Z^2} \qquad [28]$$

Together with the boundary conditions in Eq. [24], this relation shows that the discharge in a composite electrode proceeds in the same way as diffusion (according to Ficks second law) in a bounded domain $0 \leqq Z \leqq 1$ with constant flux at the two boundaries.

In the dimensionless units used above, the quantity $K/(E_l^o + E_e^o)$ is equivalent to a diffusion coefficient which in dimensioned units is

$$D_C = \frac{k}{\mathbf{F}\cdot v\cdot c^o\left(\frac{1}{\kappa_l} + \frac{1}{\kappa_e}\right)} \qquad [29]$$

To describe the discharge characteristics of the electrode at the given load a "load factor," L_c, is introduced

$$L_C = \frac{\tau_c}{\tau_D} = \frac{E_l^o + E_e^o}{K} = (1 + \beta)E_l^o/K = \frac{|i^*|\cdot l}{k}\left(\frac{1}{\kappa_e} + \frac{1}{\kappa_l}\right) \qquad [30]$$

where τ_C is the time constant for the electrode: l^2/D_C.[1] The solution of Eq. [28] can be obtained by combining solutions for the equivalent heat conduction phenomena (25) as discussed in the Appendix.

The two solutions below are written using L_C and $E_e^o = \beta \cdot E_l^o$ to demonstrate the influence of additional electronic resistance

$$X = T + \frac{E_l^o}{K}\left\{\frac{1+\beta}{2}Z^2 - \beta Z + \frac{\beta}{3} - \frac{1}{6} + \frac{2}{\pi^2}\sum_{n=1}^{\infty}\frac{(-1)^n}{n^2}\exp[-n^2\pi^2 T/L_C]\,[\beta\cos n\pi Z - \cos n\pi(1 - Z)]\right\} \qquad [31]$$

and[2]

$$X = 2\frac{E_l^o}{K}\frac{\sqrt{T}}{L_C}\sum_0^\infty\left[\text{ierf}\frac{2n+1+Z}{2\sqrt{T/L_C}} + \text{ierfc}\frac{2n+1-Z}{2\sqrt{T/L_C}} + \beta(\text{ierfc}\frac{2n+Z}{2\sqrt{T/L_C}} + \text{ierfc}\frac{2n+2-Z}{2\sqrt{T/L_C}}\right] \qquad [32]$$

These relations are most conveniently treated by considering "long time" and "short time" behavior separately. To obtain an acceptable battery capacity, L_C should be less than one. For $T > L_C/3$, the sum of exponentials in Eq. [31] vanishes, giving the long time approximation

$$X = T + \frac{E_l^o}{K}\left(\frac{1+\beta}{2}Z^2 + \beta Z + \frac{\beta}{3} - \frac{1}{6}\right) \qquad [33]$$

This concentration profile is a parabola with minimum value at $Z = \beta/(1 + \beta)$. The values of X at the back and front are

$$Z = 0,\ X_0 = T + (2\beta - 1)E_l^o/6K$$
$$Z = 1,\ X_1 = T + (2 - \beta)E_l^o/6K \qquad [34]$$

Using Eq. [18] and [11], the dimensionless working potential is found as

$$E_c = E^* - KT - (E_l^o + E_e^o)/3 = E^* - KT - (1 + \beta)E_l^o/3 \qquad [35]$$

For "short time," an approximation can be obtained from Eq. [32] observing that, for small values of T/L_C, all terms except those with $n = 0$ in the summations vanish, (ierfc $1.5 < 0.01$). Also, for Z near zero, only the term with ierfc $(Z/2\sqrt{T/L_C})$, and for Z near one, only ierfc $((1 - Z)/2\sqrt{T/L_C})$ remains. Hence, the short time approximation is

$$X = 2\frac{E_l^o}{K}\sqrt{\frac{T}{L_C}}\left(\text{ierfc}\frac{1-Z}{2\sqrt{T/L_C}} + \beta\ \text{ierfc}\frac{Z}{2\sqrt{T/L_C}}\right) \qquad [36]$$

showing that the profile is composed of two semi-infinite diffusion profiles starting from $Z = 1$ and $Z = 0$, respectively. They both travel inward and at $Z = \beta/(1 + \beta)$ they meet, building up the parabola given by Eq. [33]. The values of X at the back and front of the electrode are [ierfc(0) = $1/\sqrt{\pi}$]

$$Z = 0,\ X_0 = 2\frac{\beta E_l^o}{K}\sqrt{\frac{T}{\pi L_C}}$$
$$Z = 1,\ X_1 = 2\frac{E_l^o}{K}\sqrt{\frac{T}{\pi L_C}} \qquad [37]$$

Then using Eq. [11] and [18], the dimensionless working potential is

$$E_c = E^* - \frac{2}{\sqrt{\pi}}\frac{1+\beta^2}{(1+\beta)^{3/2}}\sqrt{KE_l^o\cdot T} - \frac{\beta}{1+\beta}E_l^o \qquad [38]$$

This relation demonstrates the $\sqrt{t}$ dependence, typically for semi-infinite diffusion, but it also contains a constant term for $t = 0$ which is largest for $E_l^o = E_e^o$, $(\beta = 1)$.

Equations [35] and [38] are asymptotic solutions for $T \to \infty$ and $T \to 0$, but they are both very good approximations over a large range. Equating dE_c/dT from these two expressions, a transition point is found for

$$T_t = \left[\frac{1+\beta^2}{(1+\beta)^2}\right]^2\frac{L_C}{\pi} = \frac{(1+\beta^2)^2}{(1+\beta)^3}\frac{E_l^o}{\pi K} \qquad [39]$$

and, at this point, the true value for E_C deviates less than $0.01(E_e^o + E_l^o)$ from the values calculated from Eq. [35] and [38]. Thus, these two relations cover the range $0 < T < 1 - L_C/3$ with a sufficient precision for all practical purposes.

The low potential region.—Physically, X can never exceed 1, and, thus, Eq. [35] or [38] are only valid for $T < T_{sat}$,

[1] In Ref. (11), the reciprocal of L_C was used, called Q.

[2] ierfc is the first integral of the erfc function. See Ref. (25).

where T_{sat} is found by equating X to 1 in Eq. [34] or [37]. For practical batteries, a utilization of more than 50% is usually required and hence, only the use of Eq. [34] is relevant. From this, T_{sat} is

$$\beta \leqq 1,\ T_{sat} = 1 - (2 - \beta)\frac{E_1^o}{6K} = 1 - \frac{2 - \beta}{6(1 + \beta)} L_C$$
$$\beta \geqq 1,\ T_{sat} = 1 - (2\beta - 1)\frac{E_1^o}{6K} = 1 - \frac{2\beta - 1}{6(1 + \beta)} L_C \quad [40]$$

For $\beta = 0$ and $\beta \to \infty$, T_{sat} is $1 - L_C/3$, and for $\beta = 1$, T_{sat} is $1 - L_C/12$. At T_{sat} the insertion compound becomes saturated either at the surface (for $\beta < 1$) or at the current collector ($\beta > 1$). For $\beta = 1$, the saturation occurs simultaneously at the surface and at the current collector.

However, the discharge of the inner parts of the electrode can continue for $T > T_{sat}$. For $\beta < 1$, due to the transport of M^+ in the ionic conducting network to the nonsaturated inner parts, and for $\beta > 1$, correspondingly through transport of electrons in the electronic conducting network of (saturated) insertion compound. In this way the electrode can, in principle, be discharged to 100% utilization.

This part of the discharge is characterized by a boundary between the saturated and still active part of the electrode; the boundary moving inwards for $\beta < 1$. From this boundary on, the electrode reaction proceeds as usual and Eq. [24] will apply. However, the boundary condition $dE/dZ = -E_1^o$ should now be applied to the moving boundary between the saturated and the active part of the electrode. For $\beta > 1$, saturation starts at the current collector. The total current is now carried by the electronic conducting network to the boundary, which is now moving forward but still subjected to the boundary condition $dE/dZ = E_e^o$. For $\beta = 1$, two boundaries starting at each end move against each other. In Fig. 5, we have depicted the development of concentration profiles in the electrode with T for different characteristic values of β.

A simple analytical solution of Eq. [24] with moving boundary conditions has not been found. However, an approximate solution for the position of the boundary can be found if one assumes that the shape of the concentration profile remains parabolic as for $T < T_{sat}$. This appears reasonable when $1 - T_{sat}$ is small.

The analytical solutions are only simple for E_e^o or $E_1^o = 0$ or in the symmetrical case $E_e^o = E_1^o$. For $\beta = 0$ let the boundary between the outer saturated and the inner active region be at $Z = Z^*$. Then, using the boundary conditions at $Z = 0$ and $Z = Z^*$ and the assumption about a parabolic shape, the concentration profile ($0 \leqq Z \leqq Z^*$) is found to be

$$X = \frac{E_1^o Z^2}{2K Z^*} - \frac{E_1^o}{2K} Z^* + 1 \quad [41]$$

As the total inserted amount is T, Z^* can be found from

$$T = \int_0^{Z^*} X dZ + 1 - Z^* \quad [42]$$

resulting in

$$Z^* = \sqrt{3K(1 - T)/E_1^o} \quad [43]$$

For $\beta = 1$ ($E_e^o = E_1^o$), we have two boundaries, Z_1^* and Z_2^*, symmetrical about $Z = \frac{1}{2}$. With the same procedure as above, we get

$$Z_1^* = \tfrac{1}{2} + \sqrt{3K(1 - T)/2E_1^o}$$
$$Z_2^* = \tfrac{1}{2} - \sqrt{3K(1 - T)/2E_1^o} \quad [44]$$

At the boundaries, the local electrode potential according to Eq. [11] is $E^* - K$. If $E_e^o = 0$, we get the working potential directly as

$$E_c = E^* - K - E_1^o(1 - Z^*) \quad [45]$$

And for $E_e^o = E_1^o$ ($\beta = 1$)

$$E_c = E^* - K - E^o(1 - Z^*) - \frac{\mathbf{F}}{RT}\int_{Z_1^*}^{Z_2^*} \pi dZ \quad [46]$$

Inserting Eq. [43] in [45] and Eq. [44] in [46] and evaluating the integral as for Eq. [18], we get as a common result

$$E_c = E^* - K - E_1^o(1 - \sqrt{3K(1 - T)/(\beta + 1)E_1^o}) \quad [47]$$

valid for $\beta = 0$ and 1.

The final working potential at $T = 1$ is thus estimated as

$$E_c(T \simeq 1) = E^* - K - E^o \quad [48]$$

where E^o is E_1^o for $\beta \leq 1$ or E_e^o for $\beta \geq 1$.

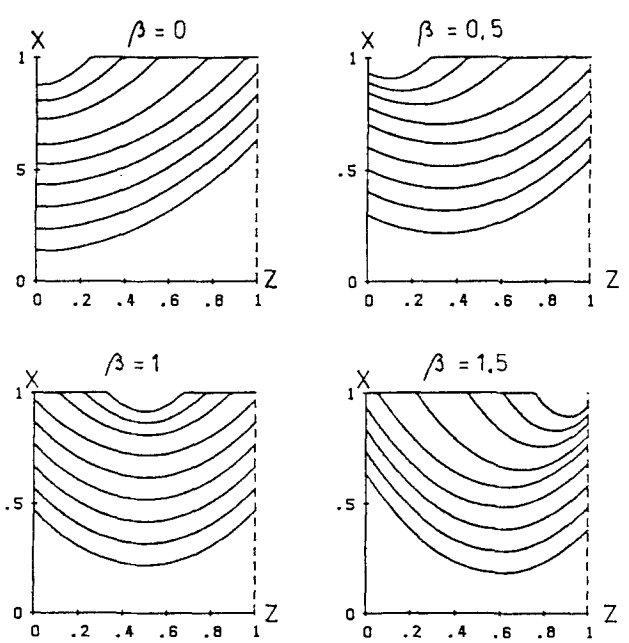

Fig. 5. Calculated concentration profiles in composite electrode. Different values of $\beta = \kappa_l/\kappa_e$ as indicated. E_1^o/K kept constant. Counted from lowest value of X, T = 0.3, 0.4, 0.5, 0.6, 0.7, 0.8, 0.9, 0.95, and 0.98.

Discussion

The basic Eq. [28] demonstrates that in the region where $\dot{X} < 1$ the composite electrode behaves like a nonporous insertion electrode. The apparent diffusion coefficient depends, according to Eq. [29], on the slope of the EMF curve, on the conductivities, and on the specific capacity ($c^o \cdot v$) of the electrode.

Using available data for the TiS_2/Li_3N combination,[3] a value of $D_c \cong 10^{-5}$ cm^2 s^{-1} is obtained at 170°C. This relatively high value allows construction of batteries with a high materials utilization and a good packing density even at heavy loads.[4]

To illustrate this further, the discharge curve, *i.e.*, the working voltage, ϵ_C, as a function of degree of discharge, T, can be calculated for an electrode with known values of k, ϵ_l^o, ϵ_e^o, and ϵ^*. This can be done using Eq. [38], [35], and [47], successively, observing that the discharge curve can be divided in three regions: the $\sqrt{T}$ region, the linear part, and the low potential region characterized by a $\sqrt{1 - T}$ dependence. The transition points between these regions as given by Eq. [39] and [40] are determined by the load factor L_C defined in Eq. [30]. The case $\epsilon_l^o >> \epsilon_e^o$ ($\beta = 0$) is of considerable practical interest and may serve as an illustration of the characteristic course of the discharge curve. Using dimensioned units ($k = RTK/\mathbf{F}$, $L_C = \epsilon_l^o/k$), the three regions can be described thus

[3] $C^o = 0.026$ mol cm^{-3}, $K = 22$, $\kappa_e >> \kappa_l \simeq 2.5 \cdot 10^{-3}$ Ω^{-1} cm^{-1} at 170°C, $v = 0.5$.

[4] It has been experimentally shown that although the TiS_2/Li_3N combination is thermodynamically unstable, it is kinetically stable. Batteries with TiS_2/Li_3N composite electrodes have been cycled more than 500 times (30).

$T < L_C/\pi$;

$$\epsilon_C = \epsilon^* - \frac{2}{\sqrt{\pi}}\sqrt{\epsilon_l^{\circ} k \cdot T}$$

$L_C/\pi < T < 1 - L_C/3$; [49]

$$\epsilon_C = \epsilon^* - \epsilon_l^{\circ}/3 - k \cdot T$$

$1 - L_C/3 < T < 1$;

$$\epsilon_C = \epsilon^* - k - \epsilon_l^{\circ}(1 - \sqrt{3k(1-T)/\epsilon_l^{\circ}})$$

In Fig. 6, discharge curves for $L_C = 1$ and different combinations of k and ϵ_l° are depicted. The effect of an additional electronic resistance ($\beta > 0$) is illustrated in Fig. 7. Contrary to the case for $\beta = 0$, there is according to Eq. [38] an initial ohmic voltage drop: $\epsilon_e^{\circ}/(1 + \beta)$. In a complete battery, this will be observed in addition to the voltage drop across the separator electrolyte. The $\sqrt{T}$ part of the curve is flattened due to the factor $(1 + \beta^2)/(1 + \beta)^{3/2}$ in Eq. [38] (= 0.7 for $\beta = 1$). The linear part is further depressed by $\epsilon_e^{\circ}/3$, but the linear range is extended at the expense of the $\sqrt{T}$ and the $\sqrt{1 - T}$ regions, delaying the appearance of the more sloping last part of the discharge. The end-point voltage ($T \simeq 1$) is, however, the same as for $\beta = 0$ *cf.* in Eq. [48].

In general, the course and position of the discharge curve are determined by k and ϵ^*, characteristic for the insertion compound, and by the quantities ϵ_l° and ϵ_e°, which besides the electronic and ionic conductivities κ_e and κ_l, combine the influence of the discharge current, the thickness of the electrode, and the volume fraction and saturation concentration of the insertion compound.

ϵ^* and k are thermodynamic quantities given by the affinity of the cathode reaction in Eq. [2]. k in particular depends on the interactions associated with the insertion reaction. The ϵ_o's as given by Eq. [16] contain the effective conductivities κ_e and κ_l. The magnitudes of these are critical for the battery performance. It should be realized that these conductivities are effective values, including the effects of volume fraction, tortuosity, contact resistance between particles, and voids in the electrode. All this adds up to a considerable reduction in the effective conductivities compared with those of the pure substances.

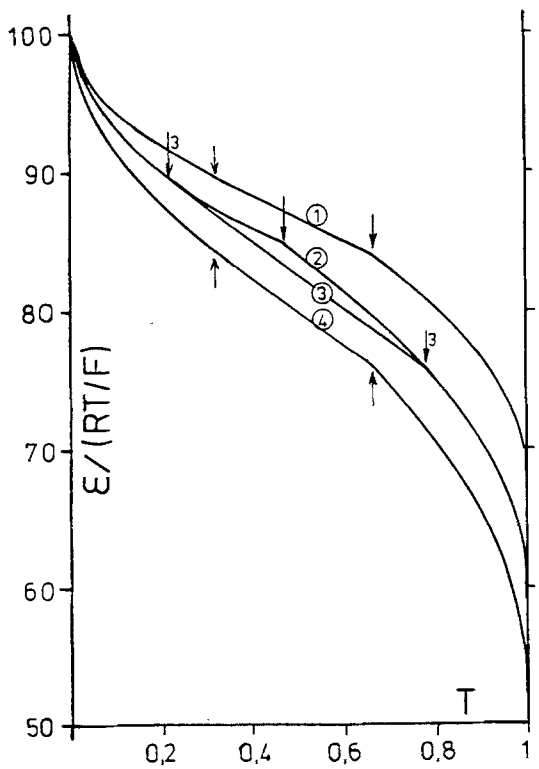

Fig. 6. Calculated discharge curves. $\kappa_e >> \kappa_l \cdot$ (1) $E_l^{\circ} = 16, K = 16$: (2) $E_l^{\circ} = 24, K = 6$; (3) $E_l^{\circ} = 16, K = 24$; and (4) $E_l^{\circ} = 24, K = 24$. Transition points indicated by arrows.

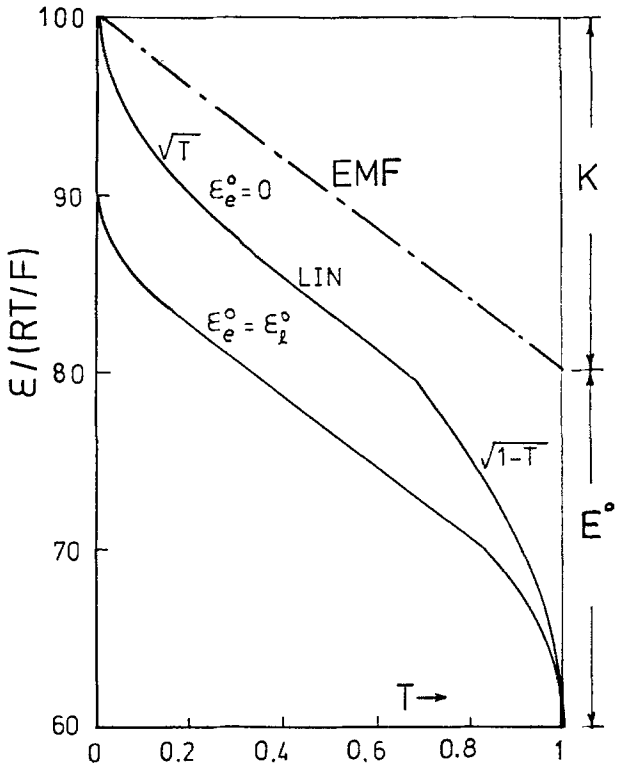

Fig. 7. Calculated discharge curves demonstrating the effect of electronic resistance. Parameters as indicated.

As the electrolyte and insertion compound particles act as nonconducting diluents for each other, some guidance as to the magnitudes of the effective values can be obtained from the study of conductivities of heterogeneous systems as carried out by Meredith and Tobias (26) and later discussed by Newman and Tiedemann (27). According to these authors, κ_l and κ_e can be estimated from the volume fractions and the conductivities of the pure substances κ_l° and κ_e° by the relations

$$\kappa_l/\kappa_l^{\circ} = (1 - v)^{\alpha};\ \kappa_e/\kappa_e^{\circ} = v^{\alpha} \quad [50]$$

where the exponent α has a value in the range $1.5 < \alpha < 2.5$. Using Eq. [50], ϵ_e° and ϵ_l° can be written as

$$\epsilon_l^{\circ} = \mathbf{F}\frac{l^2 c_o v}{\tau_D \kappa_l^{\circ}(1 - v)^{\alpha}} = -\frac{l}{\kappa_l^{\circ}(1 - v)^{\alpha}} \cdot i^*$$

and [51]

$$\epsilon_e^{\circ} = \mathbf{F}\frac{l^2 c^{\circ}}{\tau_D \kappa_e^{\circ} v^{(\alpha-1)}} = -\frac{l}{\kappa_e^{\circ} v^{\alpha}} \cdot i^*$$

From these relations, it can be estimated how the different design parameters and the discharge regime influence the course of the discharge curve and thus, the obtainable materials utilization. For example, for different loads it is obvious that the ratio l^2/τ_D should remain constant for a given electrode composition in order not to change the discharge behavior.

Due to the uncertainty present in estimates of the effective conductivities, it is certainly a safer approach to consider the effective κ's as phenomenological parameters characteristic for a given electrode composition, grain size, and fabrication technique, and to measure them directly on a sample electrode.

This can be done using blocking electrodes for M^+ ions and electrons, respectively, considering the composite as a mixed conductor, and using the methods discussed, *e.g.*, by Rickert (28). It is important in these measurements to observe the requirement of electrochemical equilibrium between the insertion compound and the electrolyte.

Alternatively, estimates of $\epsilon_e^0 + \epsilon_l^0$ and k can be found from the discharge curves when the current is chosen low enough to allow development of the linear region. In these cases, k is the slope of the linear part, while the position of the discharge curve (corrected for the potential difference across the separator) according to Eq. [35] or [49] allows determination of $\epsilon_e^0 + \epsilon_l^0$ for a given current. In cases $\kappa_e >> \kappa_l$ ($\beta = 0$), the potential difference across the separator can be found from the instantaneous voltage transient when switching the current on or off.

As mentioned above, a consequence of the immobility of the compensating charges in the electrolyte is the possibility to discharge the composite electrode until $T = 1$, as discussed in the derivation of Eq. [47]. However, the predictions which can be made for this part of the discharge are less precise than the predictions for the square root and linear regions. First it must be realized that the assumption about a linear potential/composition relation has limited validity. For $X > 0.95$, a relation like Eq. [10] is a better approximation to the potential dependence, thus causing a steeper slope of the discharge curve and a lower end-point voltage. Also for that part of the discharge, where only a small part of the electrode is active, the assumptions about equilibrium in the insertion compound particles and on the surface of these cannot be maintained because of the high final local current transfer. For $T > 0.95$ the influence of these limitations must be studied using a numerical technique as discussed in our previous paper (14).

Conclusion

The discharge behavior of a composite electrode containing a finely divided insertion electrode material can be adequately described by the ionic and electronic conductivities of the composite and the slope of the EMF/composition curve for the insertion compound.

Using reasonable approximations, the course of the discharge curve for a given electrode can be calculated analytically for a specified constant current load. Due to the immobility of the compensating charges in the solid electrolyte, theory predicts that a materials utilization near 100% can be obtained to an acceptable discharge end point.

The possibility of realizing these advantages depends on the availability of a good solid ion conductor for the inserted ion. The fulfillment of this requirement is facilitated by the possibility of operating this type of electrode at a moderately increased temperature.

Technologically, the realization of the composite electrode concept requires the development of a fabrication technique which results in a structure consisting of two contiguous networks of electrolyte and insertion compounds in intimate contact.

Manuscript submitted Feb. 24, 1983; revised manuscript received Aug. 26, 1983.

APPENDIX

The heat conduction problem (25)

$$0 \le x \le l,\ V = 0 \text{ for } t = 0$$

$$\frac{\partial V}{dx} = 0 \text{ for } X = 0;\ \frac{dV}{dx} = \frac{\mathbf{F}^0}{K} \equiv A \text{ for } x = l \qquad [A\text{-}1]$$

$$\frac{\partial V}{\partial t} = \kappa \frac{\partial^2 V}{dx^2};\ \kappa = \frac{K}{\rho c} \equiv \gamma$$

has (loc.cit.) the solutions

$$V = A\gamma \cdot t/l + A(x^2/2l - l/6 - \frac{2}{\pi^2}\sum_1^\infty \frac{(-1)^n}{n^2} \exp[-n^2\pi^2\gamma t/l^2] \quad \cos n\pi x/l)$$

and

$$V = 2A\sqrt{\gamma t}\sum_0^\infty \left(\text{ierfc}\frac{(2n+1)\,l + x}{2\sqrt{\gamma t}} + \text{ierfc}\frac{(2n+1)l - x}{2\sqrt{\gamma t}}\right) \qquad [A\text{-}2]$$

Equations [24] and [28] can be written

$$U = U(Z,T) \quad 0 \le Z \le 1;\ U(Z,0) = 0$$

$$\partial U/dZ = \alpha_1,\ Z = 0;\ \partial U/\partial Z = \alpha_2,\ Z = 1$$

$$\frac{\partial U}{\partial T} = \gamma \frac{\partial^2 U}{\partial Z^2} \qquad [A\text{-}3]$$

Let $R = R(r, T)$ and $S = S(s,T)$ be defined by

$$\frac{\partial R}{\partial T} = \gamma \frac{\partial^2 R}{\partial r^2};\quad \frac{\partial S}{\partial T} = \gamma \frac{\partial^2 S}{\partial s^2}$$

$$S = R = 0,\ T = 0;\quad s = 1 - r$$

$$\partial R/\partial r = 0,\ r = 0;\quad \partial R/\partial r = -\alpha_1,\ r = 1 \qquad [A\text{-}4]$$

$$\partial S/\partial s = 0,\ s = 0;\quad \partial S/\partial s = \alpha_2,\ s = 1$$

Then, $U = R + S$ is a solution to [A-3]. From Eq. [A-1], for $l = 1$, $x \equiv r = 1\text{-}Z$, and $A = -\alpha_1$

$$R = -\alpha_1\gamma T - \alpha_1(1/3 - Z + \frac{Z^2}{2} - \frac{2}{\pi^2}\sum_1^\infty \left[\frac{(-1)^n}{n^2} \exp[-n^2\pi^2\gamma T] \cos n\pi(1 - Z)\right])$$

And for $x \equiv s = Z$, $A = \alpha_2$

$$S = \alpha_2\gamma T + \alpha_2\left(Z^2/2 - 1/6 - \frac{2}{\pi^2}\sum\left[\frac{(-1)^n}{n^2} \exp[-n^2\pi^2\gamma T] \cos n\pi z\right]\right)$$

leading to

$$U = (\alpha_2 - \alpha_1)\gamma T + (\alpha_2 - \alpha_1)Z^2/2 + \alpha_1 Z - \alpha_1/3 - \alpha_2/6 \qquad [A\text{-}5]$$

$$-\frac{2}{\pi^2}\sum\frac{(-1)^n}{n^2}(\exp[-n^2\pi^2\gamma T][\alpha_2\cos n\pi Z - \alpha_1\cos \pi(1 - Z)])$$

or using Eq. [A-2]

$$U = 2\sqrt{\gamma T}\left[\alpha_2\sum_0^\infty\left(\text{ierfc}\frac{2n+1+Z}{2\sqrt{\gamma T}} + \text{ierfc}\frac{2n+1-Z}{2\sqrt{\gamma T}}\right) - \alpha_1\sum_0^\infty\left(\text{ierfc}\frac{2n+Z}{2\sqrt{\gamma T}} + \text{ierfc}\frac{2n+2-Z}{2\sqrt{\gamma T}}\right)\right] \qquad [A\text{-}6]$$

Inserting $\gamma = K/(E_e^0 + E_l^0) = 1/L_c$ and $\alpha_1 = -E_e^0/K = -\beta E_l^0/K$, $\alpha_2 = E_l^0/K$ in Eq. [A-5] and [A-6] gives Eq. [31] and [32].

LIST OF SYMBOLS

c^0	saturation concentration of inserted ion in insertion compound
f	interaction parameter in Eq. [10]
i^*	overall discharge/charge current density
i_e	local electronic current density
i_l	local ionic current density
i_t	transfer current per unit electrode volume
k	slope of linearized Eq. [11]
l	thickness of composite electrode
n	amount of M^+ in HM_x at saturation and also variable in Eq. [31] and [32]
t	discharge/charge time, time coordinate
x	amount of M in HM_x
v	volume fraction of insertion compound
z	length coordinate $0 \le z \le l$
D_c	apparent chemical diffusion coefficient for M^+ in composite
H	insertion compound
M^+	inserted ion

T in $RT/\mathbf{F}$, Kelvin temperature

Dimensionless Variables and Groups

E dimensionless potential, $E_j^m = \epsilon_j^m \mathbf{F}/RT$ (for significance of superscripts and subscripts see ϵ.)
K $k \cdot \mathbf{F}/RT$
L_C load factor, τ_C/τ_D
X degree of insertion, $X = x/n$
T degree of discharge, $T = t/\tau_D$
Z length coordinate, $Z = z/l$
Z^* boundary between saturated and active part of electrode

Greek Letters

α exponent in Eq. [50]
β ratio of ionic to electronic conductance and also $\beta = \epsilon_e^o/\epsilon_i^o$
ϵ insertion compound electrode potential, $\epsilon = \pi - \phi$
ϵ_θ standard potential in Eq. [10].
ϵ_o, ϵ_l ϵ at back and front of electrode, respectively
ϵ_C working potential of electrode
ϵ^* electrode potential before discharge
ϵ_e^o $-i^* \cdot l/\kappa_e$
ϵ_i^o $-i^* \cdot l/\kappa_l$
ϕ Galvani potential in electrolyte
κ_e, κ_l effective electronic, ionic conductivities in composite (bulk values)
κ_e^o, κ_l^o electronic, ionic conductivities of insertion compound and solid electrolyte
π Fermi potential in insertion compound ($\pi = -\bar{\mu}_e/\mathbf{F}$)
τ_C time constant for composite electrode = l^2/D_C
τ_D stoichiometric discharge time = $-\mathbf{F} \cdot v \cdot c^o \cdot l/i^*$

REFERENCES

1. G. H. Newman and J. P. Kleman, *This Journal*, **127,** 2097 (1980).
2. G. H. Newman and J. P. Kleman, *ibid.*, **129,** 230 (1982).
3. A. Bottini, M. Lazzari, G. Razzini, B. Rivolta, G. De Felici, M. A. Voso, and B. Scrosati, *J. Electroanal. Chem.*, **98,** 165 (1979).
4. M. S. Whittingham, *Prog. Solid State Chem.*, **12,** 41 (1978).
5. D. W. Murphy, P. A. Christian, F. D. DiSalvo, and J. V. Waszczak, *Inorg. Chem.*, **18,** 2800 (1979).
6. L. H. Gaines, R. W. Francis, G. H. Newman, and B. M. L. Rao, 11th Intersociety Energy Conversion Engineering Conference, Stateline, NV (1976).
7. C. C. Liang, A. V. Joshi, and N. E. Hamilton, *J. Appl. Electrochem*, **8,** 445 (1978).
8. J. R. Rea, G. S. Kelsey, H. C. Kuo, and M. Kallianidis, *Solid State Ionics*, **3/4,** 267 (1981).
9. S. Atlung, *Prog. Batt. Solar Cells*, **2,** 96 (1979).
10. R. Jasinski, in "Advances in Electrochemistry and Electrochemical Engineering," Vol. 8, P. Delahay and C. W. Tobias, Editors, p. 291 (1972).
11. S. Atlung, K. West, and T. Jacobsen, *This Journal*, **126,** 1311 (1979).
12. S. Atlung, K. West, and T. Jacobsen, in "Materials for Advanced Batteries," D. W. Murphy, J. Broadhead, and B. C. H. Steele, Editors, p. 275, Plenum Press, New York (1980).
13. K. West, T. Jacobsen, B. Zachau-Christiansen, and S. Atlung, Extended Abstract A 11, 32nd ISE Meeting, Dubrovnik (1981).
14. K. West, T. Jacobsen, and S. Atlung, *This Journal*, **129,** 1480 (1982).
15. J. E. Oxley and B. B. Owens, in "Power Sources 3. Proceedings of the 7th International Power Sources Symposium," D. H. Collins, Editor, p. 537, Oriel Press, Newcastle (1971).
16. C. C. Liang and L. H. Barnette, *This Journal*, **123,** 453 (1976).
17. M. B. Armand, J. M. Chabagno, and M. J. Duclot, in "Fast Ion Transport in Solids," Vashista *et al.*, Editors, p. 131, Elsevier, Amsterdam (1979).
18. S. Atlung, S. Skaarup, B. Zachau-Christiansen, and K. West, Progress Report No. 2, Advanced Battery Design, EEC Contract EE/E2/429/80/DK/H (1982).
19. J. S. Newman and C. Tobias, *This Journal*, **109,** 1183 (1962).
20. J. de Levie, in "Advances in Electrochemistry and Electrochemical Engineering," Vol. 6, P. Delahay and C. W. Tobias, Editors, p. 329 (1967).
21. M. Armand, Thesis, Grenoble (1978).
22. A. J. Berlinsky, W. G. Unruh, W. R. McKinnon, and R. R. Haering, *Solid State Commun.*, **31,** 135 (1979).
23. T. Jacobsen, K. West, and S. Atlung, *Electrochim. Acta*, **27,** 1007 (1982).
24. J. J. Coleman, *Trans. Electrochem. Soc.*, **90,** 545 (1946).
25. H. S. Carslaw and J. C. Jaeger, "Heat Conduction in Solids," 2nd ed., p. 112, 310, Oxford, London (1959).
26. R. E. Meredith and C. W. Tobias, in "Advances in Electrochemistry and Electrochemical Engineering," Vol. 2, P. Delahay and C. W. Tobias, Editors, p. 15 (1965).
27. J. Newman and W. Tiedeman, *AIChE J.*, **21,** 25 (1975).
28. H. Rickert, "Einführung in die Eledtrochemie fester Stoffe," p. 107, Springer, Berlin (1973).
29. K. West, T. Jacobsen, B. Zachau-Christiansen, and S. Atlung, *Electrochim. Acta*, **28,** 97 (1983).
30. B. Knutz and S. Skaarup, 4th Internat. Conf. Solid State Ionics, Grenoble (1983).

Technical Notes

Rare Earth-Activated Niobates

W. A. McAllister

North American Philips Lighting Corporation, Bloomfield, New Jersey 07003

Alkaline earth niobate phosphors were described some time ago (1, 2), the best materials being calcium and cadmium niobates ($Ca(Cd)Nb_2O_6$) emitting in the blue and having the columbite structure. Other niobates with intrinsic blue emission are based on the fergusonite structure (3), *e.g.*, yttrium niobate ($YNbO_4$), and have been shown to be good hosts for activation by other rare earths. Energy is transferred from host to activator giving, in the case of Eu^{+3}, emission largely that of the latter species. Since there were no reports of a similar role for the calcium or cadmium niobates, we have investigated the luminescence characteristics of these materials, their solid solutions, and rare earth activated materials derived therefrom.

*Electrochemical Society Active Member.

Experimental

Phosphors were prepared by reacting SL grade calcium carbonate (GTE) and cadmium oxide (99.99% American Metals and Chemicals) with optical grade Kawecki-Berylco niobium pentoxide; rare earths, when present, were 99.99% Molycorp oxides. Firing was in air or nitrogen (Tb-activated materials only) for 2h at 1100°-1400°C, the higher temperature being required for high calcium [>50 m/o (mol percent)] members of the series. A slight excess of Nb_2O_5 was also required in these latter formulations to suppress formation of the $Ca_2Nb_2O_7$ structure (4).